International Journal of Chemical, Materials and Biomolecular Sciences
ISSN: 2415-6620
Vol:9, No:5, 2015

ORR Activity and Stability of Pt-Based Electrocatalysts in PEM Fuel Cell

S. Limpattayanate, M. Hunsom

***Abstract*—**A comparison of activity and stability of the as-formed Pt/C, Pt-Co and Pt-Pd/C electrocatalysts, prepared by a combined approach of impregnation and seeding, was performed. According to the activity test in a single Proton Exchange Membrane (PEM) fuel cell, the Oxygen Reduction Reaction (ORR) activity of the Pt-M/C electrocatalyst was slightly lower than that of Pt/C. The $j_{0.9\ V}$ and $E_{10\ mA/cm^2}$ of the as-prepared electrocatalysts increased in the order of Pt/C > Pt-Co/C > Pt-Pd/C. However, in the medium-to-high current density region, Pt-Pd/C exhibited the best performance. With regard to their stability in a 0.5 M H_2SO_4 electrolyte solution, the electrochemical surface area decreased as the number of rounds of repetitive potential cycling increased due to the dissolution of the metals within the catalyst structure. For long-term measurement, Pt-Pd/C was the most stable than the other three electrocatalysts.

***Keywords*—**ORR activity, Stability, Pt-based electrocatalysts, PEM fuel cell.

I. Introduction

PROTON EXCHANGE MEMBRANE (PEM) fuel cells are currently recognized as the most competitive candidate to replace traditional forms of power conversion due to their various advantages including that they have zero emissions, a high efficiency and a relatively simple design and operation [1]-[4]. They are able to meet the transportation and stationary power requirements owing to their low operating temperature, quick start, light weight and high power density [5]. However, the commercialization and utilization of PEM fuel cells is still not currently widespread because of two major technical gaps: their high cost and low reliability and durability [6].

Practically, highly dispersed platinum (Pt) crystallites on a conductive carbon support (*ex*. Vulcan XC-72) is utilized in a fuel cell because Pt possesses a high exchange current density for both the oxidation and reduction reactions in the fuel cell, a high resistance to chemical attack, excellent high-temperature characteristics and stable electrical properties [7]. Despite these advantages of Pt electrocatalysts in PEM fuel cells, several drawbacks to Pt based catalysts are still observed, including their sensitivity to contaminants, almost completed four-electron reduction reactions, and Pt dissolution [6]. Additionally, Pt is a high cost metal in demand for other applications and the world's supply of Pt is limited, resulting in a high production cost for fuel cells.

S. Limpattayanate is with the Fuels Research Center, Department of Chemical Technology, Faculty of Science, Chulalongkorn University, 254 Phayathai Road, Bangkok 10330, Thailand (e-mail: jsl_lsj@hotmail.com).
M. Hunsom is with the Center of Excellence on Petrochemical and Materials Technology (PETRO-MAT), Chulalongkorn University, 254 Phayathai Road, Bangkok 10330, Thailand (e-mail: mali.h@chula.ac.th)

Typically, there are three procedures to reduce Pt catalyst consumption in a fuel cell; (i) develop new Pt-based catalysts that have a higher mass activity; (ii) improve the catalyst layer structure/microporous layer/diffusion media/flow field design and (iii) improve the durability of the catalyst and support [8]. For the past 10 years, several classes of less precious and non-precious metal catalysts for PEM fuel cell cathodes have been under intensive study to try to attain a cost-effective, active and stable electrocatalyst for PEM fuel cells. These have included Ru, Pd, Au and Ag [9]-[11], chalcogenides [12]-[16], nitrides [17], [18], functionalized carbons [19]-[22] and the macrocyclic non-precious electrocatalysts [13], [23]-[30]. However, these approaches are still in the research stages and are currently far from being established let alone commercially viable. Another strategy is the development of the bimetallic alloy (Pt-M) electrocatalysts. Several previous works have pointed out that the ORR activity of Pt catalysts can be enhanced by the presence of a composite metal (M) in Pt-M alloy catalysts because the composite metal can modify the geometrical structure of the Pt metal via decreasing the Pt-Pt bond distance [31], dissolution of the more oxidizable alloying component [32], and changing the surface structure [33] or the electronic structure by increasing the Pt *d*-electron vacancy [34]. Indeed, the catalytic activity and the tolerance to chemical substance depends not only on the nature of the Pt (*ex*. Pt-Pt distance, metal particle size and surface structure), but also on the second metal [6]. Some authors have suggested that the type of the composite metal affects the stability of the Pt-alloy in an acid environment [35]-[37]. Accordingly, the relationship between the activity-stability and the composition of Pt alloys was reported to fall into one of four categories: (i) highly corrosive and highly active (M = Fe, Co, V or Mn), (ii) corrosive and highly active (M = Zn, Cu, Mo or Ni), (iii) stable, but less active (M = Zr, Cr or Ta) and (iv) stable and active (M = W or Ti) [38]. In some contrast, [39] suggested that the stability of a Pt-M alloy electrocatalyst did not depend on the type of the composite metal, but rather on the degree of alloying and the metal particle size. For example, Pt-Cr and Pt-Co are usually considered more stable than Pt-V, Pt-Ni and Pt-Fe because Cr and Co form a higher degree of alloying with Pt than V, Ni and Fe. In spite of some contradictory results on the effect of the composite metal on the resultant Pt-M catalyst stability, it is clear from the ORR activity that the presence of the composite metal enhances the stability of the Pt-M alloy electrocatalyst compared to Pt ones [40]-[46].

Based upon our previous reports [7], [47]-[50], it appeared that the preparation of Pt-Co/C and Pt-Pd/C electrocatalysts by the combined process of impregnation and seeding provided

both a more uniform dispersion of the metal particles on the catalyst surface and a smaller size of the electrocatalyst particles compared with those produced without the seeding approach. In 2012, our group reported that Pt-Pd/C showed a higher performance in single fuel cell under H_2/O_2 condition compared with Pt/C and Pt-Co/C electrocatalysts, while Pt-Co/C exhibited the better stability in acid electrolyte (0.3 M H_2SO_4) [51]. However, due to the electrocatalyst was loaded on gas diffusion layer (GDL) and the loss of catalyst during the mixing stage due to the precipitation of transition metals, the obtained performance was still low (218 mW/cm^2). Thus, the new task was carried out with more effort in order to improve the activity and stability of the obtained electrocatalyst. In this works, various strategies were carried out. For example, the electrocatalyst was loaded on membrane instead of GDL; the mixing stage of metal precursor was carried under the heating condition to avoid the precipitation of transition metal.

II. Experimental

A. Preparation of Electrocatalysts and Morphology Characterization

During the preparation of each electrocatalyst, the two elementary steps of seeding and impregnation were carried out [47]. For the Pt/C electrocatalyst, 0.1 g of the treated carbon black [50] was dispersed in 3 ml of de-ionized water to get a 1% (w/v) carbon slurry, sonicated at 70°C for 1 hr and then adjusting the solution to pH 2 with 13.3 M HCl. The seeding step was conducted by mixing 7.0 ml of the Pt precursor (20 g/l H_2PtCl_6, Fluka) with the above 10 ml of carbon-black slurry and sonicated at 70°C for 30 min. The electrocatalyst ions in the aqueous solution were then reduced to Pt metal by the addition of 20 ml of 0.12 M $NaBH_4$ (98%, Alcan) and sonicated for 30 min at 70°C. The insoluble fraction was harvested by filtration of this suspension and rinsed several times with de-ionized water to eliminate the excess reducing agent. Consequently, the impregnation step was performed by dispersing the obtained carbon powder covered by the seeded Pt metal in de-ionized water, sonicated for 1 hr and then adding it to the remaining H_2PtCl_6 solution (90% (v/v)) to obtain the required electrocatalyst loading on the carbon support (40% (w/w)). The mixture was reduced by the addition of 20 ml of 0.12 M $NaBH_4$ under sonication for 30 min to obtain the catalyst powder, which settled out of the solution/suspension. The electrocatalyst suspension was filtered, and the filtrate was washed thoroughly with hot de-ionized water and dried for 2 hr at 110°C. The preparation of the Pt-Pd/C and Pt-Co/C electrocatalysts were each performed in a similar procedure to that for Pt/C except for changing the Pt precursor to the Pt-Pd precursor (3.5 ml of 20 g/l H_2PtCl_6 (Fluka) and 2.777 ml of 20 g/l $PdCl_2$ (98%, Fluka)) or Pt-Co precursor (3.5 ml of 20 g/l H_2PtCl_6 (Fluka) and 3.672 ml of a 20 g/l $CoCl_2$ ($CoCl_2 \cdot H_2O$, Kanto Chemical)), respectively, and the precursor mixing stage was carried out at 60 ^oC to avoid the precipitation of transition metals.

The morphology of all three types of the as-prepared electrocatalysts, along with the commercial Pt/C one, was characterized using X-ray diffraction (XRD) analysis on a Bruker D8-Discover machine, by scanning electron microscopy with energy dispersive X-ray analysis (SEM-EDX) on a JEOLJSM-5800LV and by transmission electron microscopy (TEM) on a JEOLJEM-2100.

B. Preparation of the Diffusion Layer, Electrocatalyst Ink and Electrocatalyst-Coated Membrane

The diffusion layer was prepared by mixing 0.5 ml of distilled H_2O with 1.334 µl of PTFE (60 wt. %, Aldrich) and sonicated at room temperature for 30 min. The mixed solution was then added to 1.0 ml of *i*-propanol (99.99% C_3H_7OH, Fisher) and sonicated again at room temperature for 30 min. The treated carbon black (18.0 mg, section *A*) was then added and sonicated at room temperature for 30 min to obtain the carbon ink, which was then coated onto a 2.25×2.25 cm gas diffusion layer (GDL) (Carbon cloth, ETEK) by brushing and then drying at 80 °C for 2 min to eliminate the excess solvent. The coating of carbon ink was repeated several times until the loading of the GDL was around 2.0 mg/cm^2. The carbon ink-coated GDL was finally dried at 300°C for 1 h at atmospheric pressure.

The electrocatalyst ink was prepared by mixing 12.5 mg Pt-C (or Pt-M/C) electrocatalyst powder with 3 ml 1,2-dimethoxyethane (98%, Fluka) and sonicated at room temperature for 30 min. The obtained mixture was added into 0.142 ml Nafion solution (5% (w/v) Nafion117, Fluka) and sonicated at room temperature for 1 h. Finally, 0.187 ml ethylene glycol (98%, Qrec) was added and sonicated at room temperature for 1 h to form the electrocatalyst ink.

The membrane electrode assembly (MEA), with a 5 cm^2 active surface area, was prepared as the catalyst-coated membrane by direct spraying with a spray gun (Crescendo, Model 175-7^{TM}) onto the pretreated membrane at 80^{o}C. Prior to spraying, the membrane was clamped vertically and then the catalyst ink was sprayed with a uniform pressure of 5 psig with air as the driving gas. The distance between the spray nozzle and film surface was fixed at around 2-3 cm. During the coating process, the spray nozzle was swept slowly from the left edge of the membrane to the right edge with a vertical angle between the spray nozzle and membrane surface of approximately 30-50°. The coating surface was left for 3-5 min. to obtain a dry layer, and the coating process was repeated several times to reach a catalyst loading of 0.15 mg/cm^2 and then dried at 80°C for 10 min. The procedure was repeated for the second membrane surface and then the obtained electrocatalyst-coated membrane was immersed in hot water (55-60°C) for 5 min to eliminate ethylene glycol and 1,2-dimethoxyethane, and then dried at 80 °C for 20 min. Finally, the membrane was assembled between two sheets of GDL (Carbon cloth, ETEK) and pressed together by a compression mold (LP20, Labtech) under 65 kg/cm^2 for 2.5 min, maintaining the temperature at 137°C.

C. Activity Test in Single PEM Fuel Cell

The obtained MEA of each electrocatalyst type with a constant active surface area of 5 cm^2 was mounted on

commercial single-cell hardware (Electrochem, Inc.) and tested in a single-cell test station. Prior to testing the cell performance, the run-in stage was carried out under atmospheric pressure with a cell temperature of around 60 °C by feeding H_2 and O_2 at 100 sccm each (100% humidity). The current was drawn at a high density (> 700 mA/cm^2) for a period of 6-12 h. Consequently, the performance of the single cell was evaluated in the form of current-density-potential curves (polarization curves), monitored by a Potentiostat/Galvanostat at 60°C and ambient pressure

D. Preparation of Test Specimens for Stability Tests

The electrocatalyst ink, prepared according to section B, was coated onto the carbon substrate (carbon cloth, ETEK) by direct spraying with a spray gun. It was first cut as a spherical sheet with diameter of 0.9 cm and mounted with a home-made measuring template. The three-probe stability test of the electrocatalysts was conducted in an acid environment (0.5 M H_2SO_4) using the as-prepared electrocatalyst-coated substrate as the working electrode, a Pt wire as the counter electrode and Ag/AgCl reference electrode. The potential cycling was carried out for 0-900 rounds (cycles) using a Potentiostat/Galvanostat (PG STATO 30, Autolab) in 300 ml of 0.5 M H_2SO_4 by varying the potential from -0.5 to +1.24 V at a scan rate of 20 mV/s with a constant agitation rate of 300 rpm.

The morphology of the three electrocatalysts, including the evaluation of the particle size and particle dispersion together with the metal content, after the stability test (900 rounds of the repetitive potential cycling) was analyzed by XRD and SEM-EDX, respectively. The characterization of the fresh sample was performed on the received catalyst powder, while that of the tested sample was performed on the powders spread over the carbon substrate.

III. Results and Discussion

Representative XRD patterns of the three types of the as-prepared electrocatalysts (Pt/C, Pt-Pd/C and Pt-Co/C) compared with the commercial Pt/C electrocatalyst are shown in Fig. 1 (a). The commercial Pt/C electrocatalyst exhibited the first peak at a 2θ value of about 24.8° in the XRD pattern, referring to the presence of the carbon support in the hexagonal structure [52]. The other four peaks are the characteristic peaks for the diffraction pattern of face-centered cubic (FCC) Pt, corresponding to the planes [111], [200], [220] and [311] at 2θ of 39.67°, 45.80°, 67.78° and 81.31°, respectively. For the as-prepared Pt/C electrocatalyst, the peaks indicating the characteristic FCC crystalline Pt corresponding to above planes were clearly observed at 39.83°, 46.30°, 67.58° and 81.46°, respectively. In the presence of Pd or Co (Pt-Pd/C and Pt-Co/C electrocatalysts), the observed diffraction peaks of Pt still demonstrated the characteristic FCC crystalline Pt, indicating that the alloy catalysts have single-phase-disordered structures (*ex.* solid solutions [53]). However, compared with the diffraction of the bulk Pt, the diffraction peaks for the Pt-Pd/C and Pt-Co/C electrocatalysts were shifted slightly to higher 2θ values (40.04°, 46.60°, 68.10° and 82.01° for Pt-Pd/C; and 40.24°, 46.99°, 68.61° and 82.49° for Pt-Co/C), which indicates the formation of the Pt-Pd/C and Pt-Co/C alloy electrocatalysts involves the incorporation of the Pd or the Co atom into the FCC structure of Pt, resulting in a contraction of the lattice. The sharpness of the peaks was observed in the sequence of Pt/C >Pt-Pd/C >Pt-Co/C, indicating the presence of a more amorphous structure in the Pt-Co/C electrocatalyst compared to other electrocatalysts. Also from the plot, no characteristic peaks of metallic Pd or Co or their respective oxides were detected in the respective Pt-M/C electrocatalysts. However, their presence cannot be formally discarded because they may be present in a very small amount or even in an amorphous form. The presence of Pd- or Co- elements/compounds in the as-prepared Pt-Pd/C and Pt-Co/C electrocatalysts is supported by the SEM-EDX analysis (Figs. 1 (b), (c)).

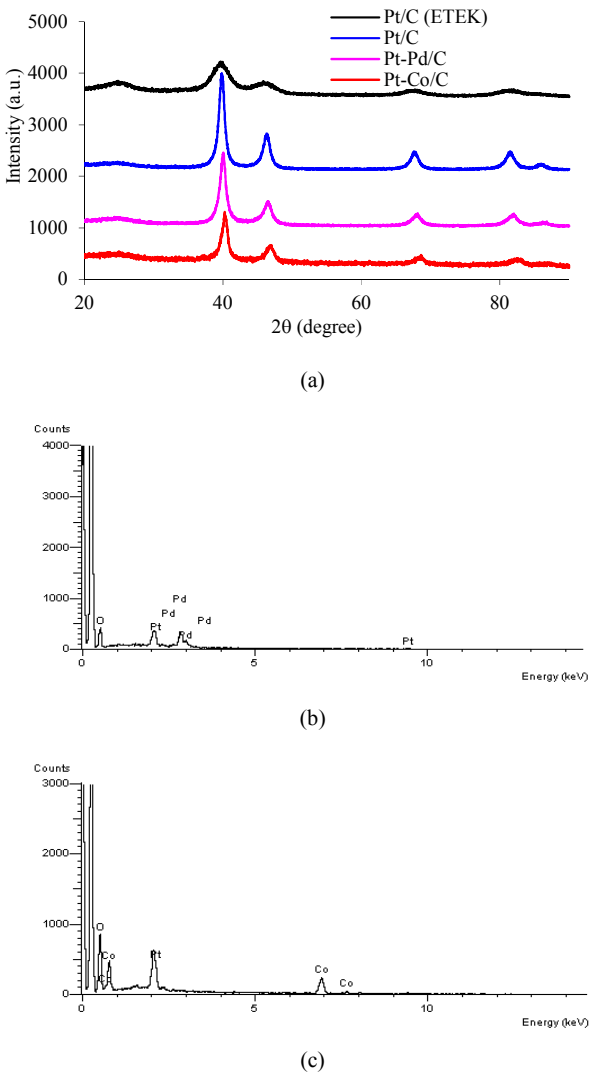

Fig. 1 (a) XRD patterns of the as-prepared electrocatalysts and the commercial Pt/C one (20 wt% ETEK), (b) SEM-EDX patterns of the Pt-Pd/C electrocatalysts and (c) SEM-EDX patterns of the Pt-Co/C electrocatalysts

To confirm the formation of the respective metal alloys, the *d*-value and lattice parameter can be estimated from XRD pattern from Bragg's law [54]. As demonstrated in Table I, it

was clearly seen that the *d*-value of both the Pt-Pd/C and Pt-Co/C electrocatalysts were smaller than that of the pure Pt/C one. Additionally, the lattice parameter of both the Pt-Pd/C and Pt-Co/C electrocatalysts were between those of pure FCC Pt (0.3923 nm), and pure FCC of either Co (0.3545 nm) or Pd (0.3891 nm), respectively, indicating the contraction of the lattice, due to the particle substitution of Pt by Pd or Co in the FCC structure [55].

TABLE I
THE *D*-VALUE, LATTICE PARAMETER AND PARTICLE SIZE OF THE DIFFERENT TYPES OF AS-PREPARED ELECTROCATALYSTS

Type Of Electrocatalyst	*d*-value (*d*, nm)	Lattice Parameter (*a*, nm)	Metal ratio (Pt: M[a])	Particle Size (*D*, nm)[b]	Dispersion (N_S/N_T, %)[c]
Pt/C	0.2261	0.3916	100	7.75	14.4
Pt-Pd/C	0.2252	0.3901	49.6: 50.4	6.78	14.8
Pt-Co/C	0.2239	0.3879	58.5: 41.5	7.39	15.4

[a] M is Pd for Pt-Pd/C and Co for Pt-Co/C
[b] Calculated from Pt[220] of XRD patterns
[c] Calculated from the particle size of XRD

The average particle size (*D*) of the electrocatalyst was then estimated from the XRD patterns according to (1), the Debye-Scherrer formula [56];

$$D = \frac{k\lambda}{\beta_{1/2}\cos\theta} \quad (1)$$

where β is the line broadening at half the maximum intensity, θ is the Bragg angle and k is a coefficient.

The smallest particle size was observed in the case of Pt-Pd/C, which was slightly (1.14- and 1.09-fold) smaller than that of the Pt/C and Pt-Co/C electrocatalysts, respectively (Table I). Additionally, the uniform dispersion of the metal elements (Pt, Pd and Co) along the carbon support was observed for all three types of the as-prepared electrode catalysts from the SEM-EDX-based element mapping (Fig. 2).

By obvious appearance, the quantity of Pt and Pd in the Pt-Pd/C electrode seemed to be almost the same while the amount of Pt in the Pt-Co/C electrode was greater than that of Co. This observation is consistent with the respective Pt : Pd and Pt : Co ratios evaluated from the EDX results (Table I). The difference in the Pt : Pd and Pt : Co ratios might be due to the difference in the standard reduction potential (E^0) of the metal ions in the system. For the former case (Pt-Pd/C), the standard reduction potential of Pd^{2+} ions (0.83 V versus SHE) is slightly greater than that of Pt^{2+} ions (0.73 V versus SHE), resulting in a faster reduction of Pd ions on the carbon substrate. In the latter case (Pt-Co/C), the standard potential of Co^{2+} (-0.28 V versus SHE) is much lower than that of Pt^{2+}, resulting in a slower reduction of Co^{2+} ions in comparison to that of Pt^{2+} ions.

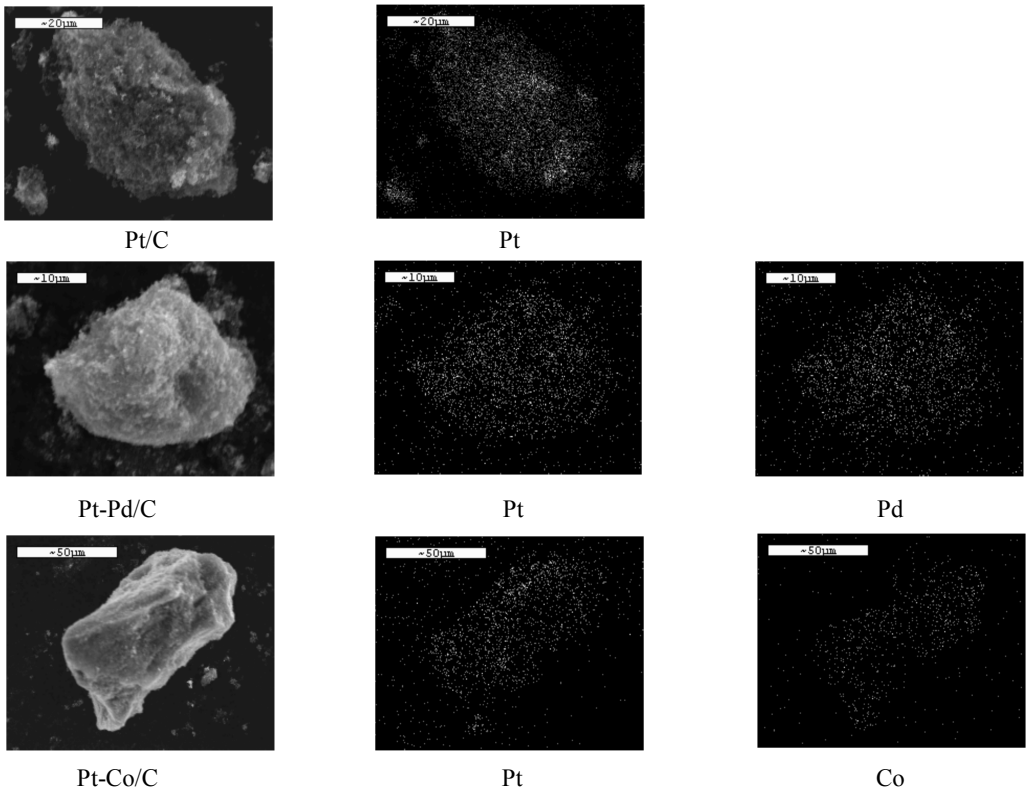

Fig. 2 Representative SEM images (general morphology) and SEM-EDX based element mapping for Pt, Pd and Co of the as-prepared electrocatalysts

The particle dispersion was estimated according to (2)-(4) [57], where N_T is the total number of atoms, N_S is the number of surface atoms, l is the number of layer, a is the lattice parameter and d is the particle size of electrocatalyst.

$$N_T = \frac{2\pi}{3}\left(\frac{d}{a}\right)^3 \quad (2)$$

$$N_T = \left(\frac{10}{3}\right)l^3 - 5l^2 + \left(\frac{11}{3}\right)l - 1 \quad (3)$$

$$N_S = 10l^2 - 20l + 12 \quad (4)$$

The maximum dispersion level was observed in the Pt-Co/C electrocatalyst at around 15.4% (Table I), which was 1.07- and 1.04-fold higher than that of the Pt/C and Pt-Pd/C electrocatalysts, respectively. The activity of the three different as-prepared electrocatalysts was tested in a H_2/O_2 PEM fuel cell at 60°C and 1 atm. All three electrocatalysts demonstrated a different ORR activity at both low- and high-current densities (Fig. 3). The open circuit voltage of the cell made with Pt-Co/C was ~1.015 V, some 0.7 and 3.4% higher than that for Pt/C (~1.008) and Pt-Pd/C (~0.98 V), respectively. This may be due to the fact that the high catalyst dispersion helped to hinder the crossover of fuel from the anode to the cathode through the membrane pin-holes. Considering the activation-controlled region at a low current density (< 100 mA/cm^2), the smallest drop in the cell potential was observed in the fuel cell with the Pt/C electrocatalyst, with the two other electrocatalysts being essentially the same as each other with a larger drop in the cell potential. In terms of the geometric surface area, the ORR activity can be approximated by the current density at 0.9 V ($j_{0.9\ V}$) or the potential at 10 mA/cm^2 ($E_{10\ mA/cm^2}$) [55]. The activity of both Pt-M/C electrocatalysts was slightly lower than that of the Pt/C one. The $j_{0.9\ V}$ and $E_{10\ mA/cm^2}$ of the as-prepared electrocatalysts increased in the order Pt/C > Pt-Co/C > Pt-Pd/C (Table II), which might be due to the presence of the different Pt contents in each electrocatalyst. That is, the Pt contents in the Pt-Pd/C and Pt-Co/C electrocatalysts were 49.6% and 58.5%, respectively, of that in the Pt/C electrocatalyst, with a drop in the catalytic activity of around 62.8% and 52.5% (based on current density) and 2.63% and 3.28% (based on voltage), respectively. Within the two Pt-M/C alloy electrocatalysts, the Pt-Co/C electrocatalyst provided a slightly higher ORR activity in comparison to that of Pt-Pd/C electrocatalyst (Table II). To explain the effect of the composite metal type on the activity of the Pt-M/C alloy electrocatalyst, it is necessary to consider the ORR mechanism. The ORR is a heterogeneous reaction, but the elementary step involves the adsorption of oxygen-containing species on the catalyst surface. Thus, the available *d*-band vacancies or number of unpaired *d*-electrons of the electrocatalyst is an important factor in the reduction reaction kinetics [58], where a high number of *d*-unpaired electrons on the catalyst results in a high coverage of oxygen-containing species [59]. In this case, Co (1.0 per atom) has a higher number of unpaired *d*-electrons in comparison to that for Pd (0.55 per atom) [60], resulting in a higher fractional coverage of oxygen species on the Pt-Co/C electrode, as well as more contraction of the lattice, measured in terms of the *d*-value and lattice parameters (Table I).

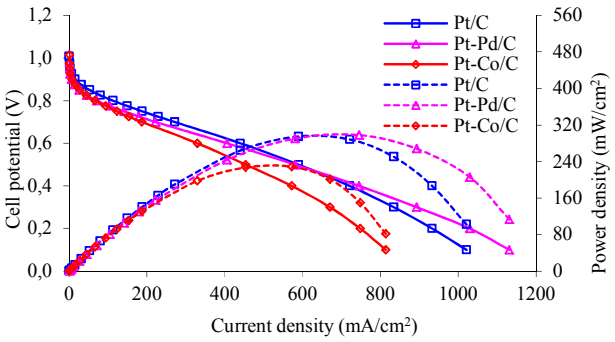

Fig. 3 Representative (—) current density-potential curve and (---) power density curve of a single H_2/O_2 PEM fuel cell of the as-prepared as-prepared electrocatalysts

TABLE II
ORR KINETIC PARAMETERS, OBTAINED FROM FITTING THE POLARIZATION DATA FROM THE $E \geq 0.8$ V REGION, OF THE THREE DIFFERENT TYPES OF ELECTROCATALYSTS.

Type of catalyst	$j_{0.9\ V}$ (mA/cm^2)	$E_{10\ mA/cm^2}$ (V)	$-b$ (mV/dec)	j_0 (mA/cm^2)	R (Ω)
Pt/C	15.42	0.914	54.90	1.02×10^{-4}	0.5189
Pt-Pd/C	5.74	0.890	55.08	4.38×10^{-5}	0.5340
Pt-Co/C	7.33	0.884	57.80	6.59×10^{-5}	0.7380

The ORR kinetic parameters of the electrode can be estimated by current density-potential data by using a non-linear least squares (NLLS) method, as expressed by (5) [60];

$$E = E_0 - b\log j - jR \quad (5)$$

where $E_0 = E_r + b\log j_0$. Here, E_r is the reversible potential for the electrode, b is the Tafel slope, R is charge transfer resistance for ORR and the electrolyte, j is the current density and j_0 is the exchange current density for the ORR. Since this equation does not include diffusion limitations other than the linear contribution, and a change in Tafel slope (b) related to the ORR is expected at potentials around 0.8 V [61], then only the region for $E \geq 0.8$ V was considered in these analyses. The fitted results are summarized in Table II. The R^2 value for all three electrocatalyst types is greater than 99.98%, indicating that the fitted model is adequate to predict the experimental data. Within the fitting error, the intrinsic Tafel slopes for the ORR were in the same range, ranging from -54.90 to -57.80 mV/dec, under the same test conditions (Table II). The maximum exchange current density (j_0), the rate constant of electron transfer at zero over potential (expressed as a current per unit area), was observed for the Pt/C electrocatalyst being some 2.33- and 1.55-fold higher than that for the Pt-Pd/C and Pt-Co/C electrocatalysts, respectively. Thus, the lowest

energy barrier for the electrochemical reaction was in the presence of the Pt/C electrocatalyst. With respect to the Pt-Pd/C and Pt-Co/C electrocatalysts, the exchange current density of Pt-Co/C was ~1.5-fold greater than that of Pt-Pd/C, indicating the faster ORR rate on the Pt-Co/C than the Pt-Pd/C electrocatalyst [62]. However, the charge transfer resistance for the ORR and the electrolyte (*R*) of Pt-Co/C were high compared to those for the Pt/C and Pt-Pd/C electrocatalysts. Additionally, over the whole range of the current density-potential curve, the performance of the Pt-Co/C electrocatalyst depleted significantly, indicating the presence of a high ohmic resistance (Fig. 3). This might be attributed to the presence of a more amorphous structure in the Pt-Co/C electrocatalyst, resulting in a slower rate of electron transfer in the catalyst structure. With regard to Pt-Pd/C, although its activity was close to that of Pt-Co/C and significantly lower than the Pt/C electrocatalyst, its performance at a medium- and high current density was significantly greater than that of either the Pt/C or the Pt-Co/C electrocatalysts (Fig. 3).

The stability of the three different types of as-prepared electrocatalysts was tested under the strongly corrosive acidic condition of 0.5 M H_2SO_4 by 900 rounds (cycles) of potential cycling between -0.5 to +1.24 V at a scan rate of 20 mV/s, and with a constant agitation rate of 300 rpm. As demonstrated in Fig. 4, the adsorption potential of the hydrogen atom onto the Pt surface (Pt-H formation, between -0.2 to +0.2 V) was not observed as a sharp peak with all three electrocatalysts, consistent with that reported previously [63]-[64]. Rather, it appeared as a broad shoulder and partially overlapped with the reduction peaks of the oxygen atom (Pt-O reduction). The desorption potential of the hydrogen atom (Pt-H oxidation, around -0.1 to 0.2 V) exhibited a strong wide peak with all three electrocatalysts. The onset desorption potential of hydrogen atoms shifted down field slightly as the number of rounds of repeat potential cycling increased, and the area under these curves decreased as the number of rounds of repeat potential cycling increased, indicating the variation in the electrocatalyst surface area [65]. More interesting current peaks that related to the Pt-OH/Pt-O formation (~ 0.6 V) were observed on the right-hand side of the positive double layer region. The magnitude of the capacitive current related to these peaks as well as to the Pt-O reduction peaks increased as the number of potential cycling rounds increased, and this was particularly the case for the two Pt-M/C electrocatalysts. This indicates the strong adsorption and accumulation of hydride as well as oxide layers on the Pt surface [40]. The increase in the capacitive current might be due to a higher degree of surface carbon oxidation with potential-holding time [63].

The electrochemical surface area (ESA) was estimated from the H2 desorption peak of the CV curve [51]. The original ESAs of the Pt/C, Pt-Pd/C and Pt-Co/C electrocatalysts were 29.9, 35.2 and 59.5 m^2/g, respectively. During the early period of potential cycling the ESAs of Pt/C and Pt-Pd/C initially increased sharply until they reached unity after 10 and 20 rounds which correspond to the maximum ESA values of 41.0 and 39.9 m^2/g, respectively. This initial increase in the ESA is due to the initial wetting of the thin Nafion layer covering the catalyst particles [41]. After saturation of the active material with the electrolyte, the ESA started to decrease with increasing rounds of potential cycling. In contrast, this initial increase in the ESA (wetting behavior) was not observed for the Pt-Co/C electrocatalyst, presumably since it has a much faster wetting behavior.

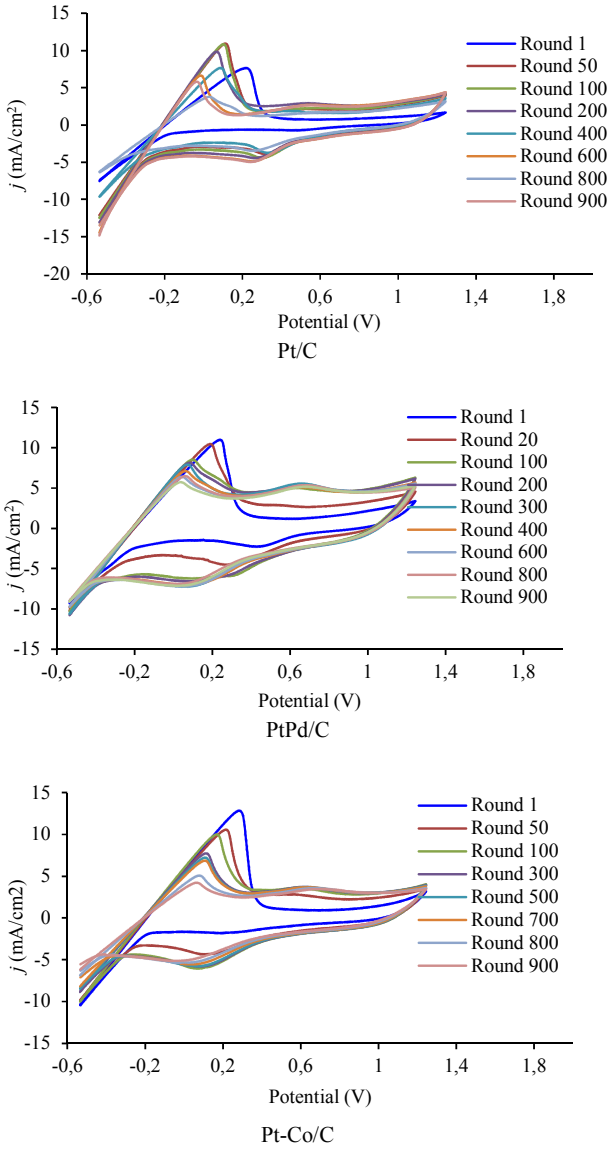

Fig. 4 CV curves of the as-prepared electrocatalysts at a metal loading of 0.15 mg/cm^2 after the indicated number of round of sequential potential cycling in 0.5 M H_2SO_4 at a scan rate of 20 mV/s

As clearly seen in Fig. 5 (a), the ESA decreased as a function of the number of repetitive potential cycling. A sharper decrease in the ESA over the whole range (0-900

rounds) of potential cycling was observed for the Pt/C electrocatalyst compared to the two Pt-M/C electrocatalysts, where the normalized ESA level dropped by almost 25% and 50% of the initial level after 300 and 500 rounds of potential cycling, respectively. The maximum loss of ESA during the early period of this stability test was observed in the case of Pt-Co/C, dropping almost 20%, 30% and 40% of the initial level after 100, 200 and 400 rounds of potential cycling, respectively, although from 200 rounds, the rate of ESA loss was reduced such that after 400 rounds, a greater ESA loss was observed with the Pt/C electrocatalyst. Throughout the 900 round stability test, the Pt-Pd/C electrocatalyst exhibited the smallest decrease in the ESA, being reduced by 25% of the initial level after 550 rounds of potential cycling and reaching a constant ESA value (~36% loss) after 800 rounds. After 900 rounds of potential cycling, the decrease in the ESA for the Pt/C, Pt-Pd/C and Pt-Co/C electrocatalysts were around 77%, 38% and 53%, respectively, which corresponded to a residual ESA of those electrocatalysts of around 9.5, 21.7 and 28.0 m^2/g, respectively. The potential loss due to the variation in the ESA was then estimated by using a modified Bulter-Volmer equation, previously reported [66]-[68]. The magnitude of the potential loss due to the loss of ESA was in the order of Pt-Co/C >Pt/C >Pt-Pd/C during the first 400 rounds of potential cycling with a loss of 12.66, 10.36 and 8.05 mV, respectively (Fig. 5 (b)). However, from 500 rounds the order of potential loss was changed. The greatest potential loss was then observed with the Pt/C electrocatalyst, while the lowest loss was with the Pt-Pd/C electrocatalyst. Thus, after 900 rounds the potential loss of the Pt/C, Pt-Pd/C and Pt-Co/C electrocatalysts were 34.8, 14.3 and 18.9 mV, respectively.

During the stability test (repeated potential cycling) the catalysts as well as the carbon support faced extremely corrosive conditions that result in the corrosion of the carbon support and also dissolution of the catalyst [41], [43]-[44]. Accordingly, the decrease in the ESA of the Pt/C electrocatalyst would result from Pt dissolution, re-deposition on the catalyst surface and Pt migration through the surface [41]. The dissolved Pt^{2+} ions can be re-deposited on the Pt surface, resulting in the formation of larger less dispersed Pt nanoparticles, a phenomenon known as Ostwald ripening [69]. However, in the presence of the transition metal or second metal in Pt/C structure (i.e. Pt-M/C), the loss of the Pt ESA decreased because the second metal helps to reduce the Pt mobility on the supporting material, and so results in a stronger bonding of the alloying metal atoms to the carbon powder, and in turn prevents sintering [40], [70]. Also, the incorporation of Co onto the Pt catalyst can reduce Pt dissolution and migration during the course of operation and so result in an increased Pt-Co/C stability compared to that for the Pt/C electrocatalyst [67]-[71]. In the case of the Pt-Pd/C electrocatalyst, the presence of Pd particles helps to reconfigure the Pt-C interaction [72], and so reduce the loss of Pt ESA in the Pt-Pd/C electrocatalyst from particle sintering.

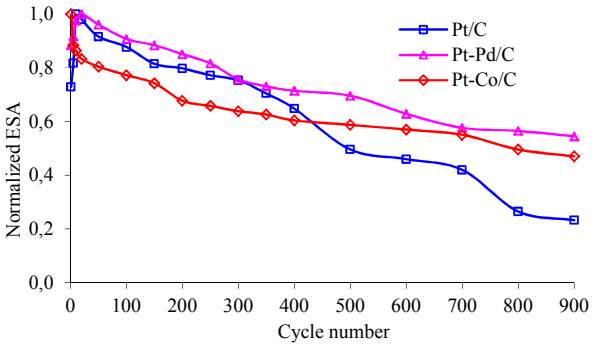

(a)

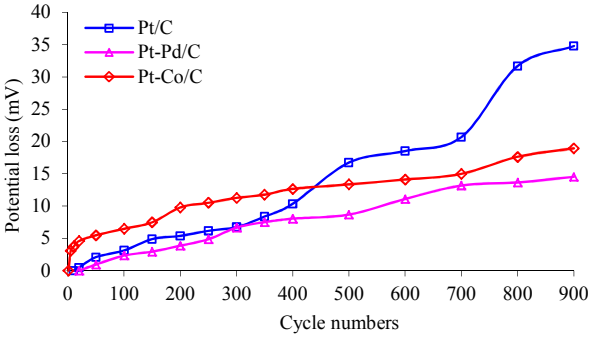

(b)

Fig. 5 (a) Normalized ESA (normalized to the maximum surface area), (b) the potential loss, of the as-prepared electrocatalysts at a metal loading of 0.15 mg/cm^2 after the indicated number of rounds (cycle numbers) of repeated potential cycling in 0.5 M H_2SO_4 at a scan rate of 20 mV/s

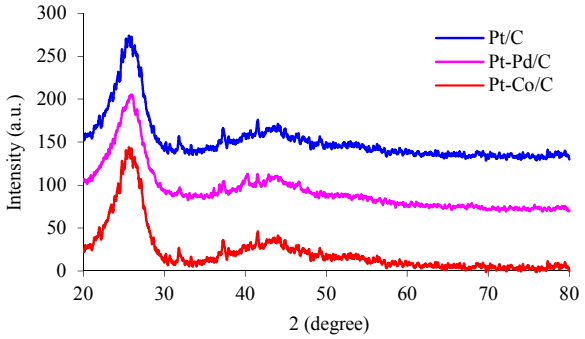

Fig. 6 Representative XRD patterns of the electrocatalysts after the stability test (900 rounds of repetitive potential cycling in 0.5 M H_2SO_4)

Representative XRD patterns of the Pt/C, Pt-Pd/C and Pt-Co/C electrocatalysts after the stability test of 900 rounds of repetitive potential cycling are shown in Fig. 6. A similar XRD pattern was observed for all three electrocatalyst types, where the main diffraction peaks observed (2θ of 24.8°) were associated with the hexagonal structure of carbon black. Compared to the as-prepared samples, the increase in the magnitude of the carbon peak intensity for the samples after

the stability test (Fig. 6) can be explained by the contribution of the carbon on the microporous layer of the carbon substrate. No sharp characteristic diffraction peaks of the Pt FCC structure were observed. The mean particle sizes of all tested electrocatalysts were also estimated by means of the Scherrer equation. To avoid the overlapping of peak Pt [111] with carbon signal, the Pt particle size was to be calculated from Pt [220]. As expected, the particle size of all three electrocatalyst types increased after the stability test (900 rounds of potential cycling), increasing approximately 2.6-, 6.1- and 30.3-fold compared to the fresh electrocatalysts. In addition, from the SEM-EDX analysis, a surface-enrichment with Pt was observed after the repetitive potential cycling. That is, the average composition of Pt : Pd and Pt : Co were changed to 87.1 : 12.9 and 96.6 : 3.4, respectively. This suggests the loss of ESA of the Pt-Pd/C and Pt-Co/C electrocatalysts involved the dissolution of Pd, Co and Pt from small-sized alloy particles and the re-deposition of Pt on the surface of larger particles, consistent with [73].

As demonstrated in SEM-EDX based element mapping, after the 900 rounds of potential cycling the Pt particles in the Pt/C and the two Pt-M/C electrocatalysts were non-uniformly distributed on the carbon substrate (Fig. 7). A slight agglomeration of Pt particles was observed in all cases. With respect to the second metal (Pd or Co), surprisingly, a more uniform distribution of the Pd or Co in the Pt-Pd/C or Pt-Co/C electrocatalyst, respectively, was clearly observed. This indicated that the dissolved Pt ions can be re-deposited on the Pt surface, resulting in the formation of larger Pt nanoparticles with a reduced distribution pattern.

According to obtained results, the Pt/C electrocatalyst still showed the best activity at 0.9 V or 10 mA/cm^2, similar to [51]. The Pt-Pd/C exhibited the higher peak power in single PEM fuel cell under H_2/O_2 environment than that of Pt/C and Pt-Co/C electrocatalysts during the whole cell potential range. However, the inconsistent results with previous work were observed during the stability test. The Pt-Pd/C exhibited a better stability than Pt/C and Pt-Co/C, while, in previous work, the Pt-Co/C had a better stability than Pt/C and Pt-Pd/C. This might be attributed to the change of catalyst preparing condition, resulting to the alternation of metal composition in electrocatalyst structure. For the whole results, all electrocatalysts prepared in this work exhibited more activity and stability than those in [51]. This might be due to the fact that the coating of electrocatalyst on membrane provided a good contact between the catalyst layer and membrane, leading to the increase in the electrochemical active area and three-phase boundary [48]. Also, the presence of ethylene glycol in catalyst structure can increase the stability of electrocatalyst during coating because of its high boiling point [74]. In addition, the electrode ink mixed with ethylene glycol as the dispersion agent had higher Pt active area.

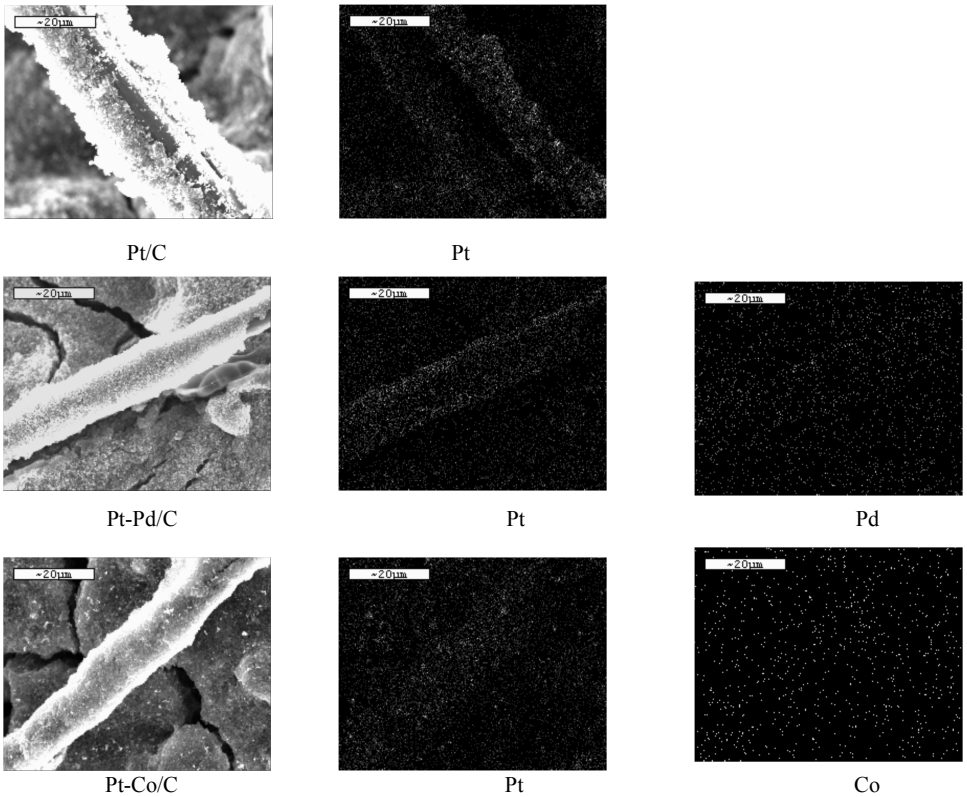

Fig. 7 Representative SEM images (general morphology) and SEM-EDX based element mapping for Pt, Pd and Co of all electrocatalysts after the stability test (900 rounds of repetitive potential cycling in 0.5 M H_2SO_4)

IV. Conclusion

Pt-M/C (M = Pd or Co) electrocatalysts were successfully prepared by a combined approach of impregnation and seeding via a low temperature reduction method. Both types of electrocatalyst demonstrated the characteristic diffraction pattern of FCC Pt. Compared with the diffraction for bulk Pt/C, the diffraction peaks for the Pt-Pd/C and Pt-Co/C electrocatalysts were shifted slightly to higher 2θ values, indicating the formation of an alloy involving the incorporation of the Pd or Co atoms into the Pt FCC structure. According to the ORR activity test in a single fuel cell under a H_2/O_2 environment, the Pt/C electrocatalyst demonstrated a higher current density at 0.9 V (or potential at 10 mA/cm^2) compared to that for the Pt-Pd/C and Pt-Co/C electrocatalysts. The Pt-Co/C electrocatalyst gave a slightly higher ORR activity in comparison to that of Pt-Pd/C electrocatalyst, due to its better electronic properties (*ex*. *d*-band vacancies). However, in the medium-to-high current density region, the Pt-Pd/C electrocatalyst demonstrated the best performance with a peak power of 298 mW/cm^2. According to the stability test in 0.5 M H_2SO_4, the ESA of all three different types of electrocatalyst decreased with increasing number of rounds of the repetitive potential cycling, due to the dissolution of Pt as well as the second metals (Pd or Co) from the electrocatalyst structure. A quicker depletion of the ESA as a function of the number of potential cycling was observed for Pt/C electrocatalyst, resulting in a potential loss of around 34.8 mV after 900 rounds. Under the investigated conditions, the Pt-Pd/C electrocatalyst exhibited a better stability than the Pt-Co/C and Pt/C ones, with a potential loss of only 14.3 mV after 900 rounds of potential cycling for Pt-Pd/C, while it was around 18.9 mV for the Pt/C and Pt-Co/C electrocatalysts. Therefore, for long-term utilization, the Pt-Pd/C electrocatalyst is the most promising candidate as an electrocatalyst in low temperature fuel cells. However, more extensive studies are required in order develop a more stable Pt-Pd/C electrocatalyst, and especially to reduce the loss of ESA to less than 40% after 3,000 rounds of potential cycling, as required by the "durability-test protocols" set by The United States Department of Energy (DOE).

Acknowledgment

The authors would like to thank the Higher Education Research Promotion and National Research University Project of Thailand, the Office of the Higher Education Commission (EN276B), the Ratchadaphiseksomphot Endowment Fund (CU-Cluster-Fund) and the Chulalongkorn University Graduate School Thesis Grant for financial support. The Thai Government Stimulus Package 2 (TKK2555), under the Project for Establishment of a Comprehensive Center for Innovative Food, Health Products and Agriculture, are thanked for facility support. Also, we thank the Publication Counseling Unit (PCU) of the Faculty of Science, Chulalongkorn University, and Dr. Robert D.J. Butcher for comments, suggestions and checking the grammar.

References

[1] K. Jiao, I.E. Alaefour, X. Li, "Three-dimensional non-isothermal modeling of carbon monoxide poisoning in high temperature proton exchange membrane fuel cells with phosphoric acid doped polybenzimidazole membranes", *Fuel*, vol. 90, pp. 568-582, Feb. 2011.

[2] A. Yilanci, I. Dincer, H.K. Ozturk, "Performance analysis of a PEM fuel cell unit in a solar-hydrogen system", *Int. J. Hydrogen. Energ*., Vol. 33, pp. 7538-7352, Dec. 2008.

[3] J.H. Lin, W.H. Chen, Y.J. Su, T.H. Ko, "Effect of gas diffusion layer compression on the performance in a proton exchange membrane fuel cell", *Fuel*, vol. 87, pp. 2420-2424, Sep. 2008.

[4] YY. Tang, W. Yuan, M. Pan, Z. Li, G. Chen, Y. Li, "Experimental investigation of dynamic performance and transient responses of a kW-class PEM fuel cell stack under various load changes.", *Appl. Energ.,* Vol. 87, pp.1410-1417, Apr. 2010.

[5] X. Zhang, J. Guo, J. Chen, "The parametric optimum analysis of a proton exchange membrane (PEM fuel cell) and its load matching", *Energy,* Vol. 35, pp. 5294-5299, Dec. 2010.

[6] C.W.B. Bezerra, L. Zhang, H. Liu, K. Lee, A.L.B. Marques, E.P. Marques, H. Wang, J. Zhang, "A review of heat-treatment effects on activity and stability of PEM fuel cell catalysts for oxygen reduction reaction", *J. Power Source*., vol. 173, pp. 891-908, Nov. 2007.

[7] W. Trongchuankij, K. Pruksathorn, M. Hunsom, "Preparation of a high performance Pt-Co/C electrocatalyst for oxygen reduction in PEM fuel cell via a combined process of impregnation and seeding", *Appl. Ener*., 88, pp. 974-980, Mar. 2011.

[8] S.S. Kocha, *Electrochemical degradation: Electrocatalyst and support durability,* in: *Polymer electrolyte fuel cell degradation*, M.M. Mench, E.C. Kumbur, T. Nejat Veziroglu., Ed., Elsevier 2012.

[9] N.A. Vante, H. Tributsch, "Energy conversion catalysis using semiconducting transition metal cluster compounds", *Nature*, vol. 323, pp. 431-432, Oct.1986.

[10] J.J.L. Fernández, V. Raghuveer, A. Manthiram, A.J. Bard, "Pd-Ti and Pd-Co-Au electrocatalysts as a replacement for platinum for oxygen reduction in proton exchange membrane fuel cells", *J. Am. Chem. Soc.*, vol. 127, pp.13100-13101, Aug. 2005.

[11] V.S. Bagotsky, *Fuel cells*, Problems and Solution, Chapter 12, John Wiley & Sons, Inc. 2009.

[12] F. Yongjun, A.V. Nicolas, "Nonprecious metal catalysts for the molecular oxygen-reduction reaction", *Phys. Status Solidi* (*b*), vol. 245, pp. 1792-1806, Aug. 2008.

[13] L. Zhang, J. Zhang, D.P. Wilkinson, H. Wang, "Progress in preparation of non-noble electrocatalysts for PEM fuel cell reactions", *J. Power. Sourc*., vol. 156, pp. 171-182, Jun. 2006.

[14] D. Baresel, W. Sarholz, P. Scharner, J. Schmitz, "Transition metal chalcogenides as oxygen catalysts for fuel-cells", *Chem. Phys*., Vol. 778, pp. 608-611, 1974.

[15] D. Susac, A. Sode, L. Zhu, P.C. Wong, M. Teo, D. Bizzotto, K.A.R. Mitchell, P.R. Parsons, S.A. Campbell, "A methodology for investigating new nonprecious metal catalysts for PEM fuel cells", *J. Phys. Chem. B*, vol. 110, pp. 10762-10770, May 2006.

[16] K. Lee, L. Zhang, J. Zhang, "Ternary non-noble metal chalcogenide (W-Co-Se) as electrocatalyst for oxygen reduction reaction", *J. Electrochem. Com*., vol. 9, pp.1704-1078, Jul. 2007.

[17] H. Zhong, H. Zhang, G. Liu, Y. Liang, J. Hu, B. Yi, "A novel non-noble electrocatalyst for PEM fuel cell based on molybdenum nitride", *Electrochem. Com*., vol. 8, pp.707-712, May 2006.

[18] H. Zhong, H. Zhang, Y. Liang, J. Zhang, M. Wang, X. Wang, "A novel non-noble electrocatalyst for oxygen reduction in proton exchange membrane fuel cells", *J. Power. Sourc.*, vol. 164, pp. 572-577, Feb. 2007.

[19] F. Charreteur, F. Jaoeun, S. Ruggeri, J. Dodelet, "Fe/N/C non-precious metal catalysts for PEM fuel cells: influence of the structural parameters of pristine commercial carbon blacks on their activity for oxygen reduction", *Electrochim. Acta*, vol. 53, 2925-2938, Feb. 2008.

[20] X. Wang, J.S. Lee, Q. Zhu, L. Liu, Y. Wang, S. Dai, "Ammonia-treated ordered mesoporous carbons as catalytic materials for oxygen reduction reaction", *Chem. Mater*., vol. 22, pp. 2178-2180, Mar. 2010.

[21] J.H. Kim, A. Ishihara, S. Mitsushima, N. Kamiya, K.I. Ota, "New non-platinum cathode based on chromium for PEFC", *Chem. Lett*., vol. 36, pp. 514-515, Jan. 2007.

[22] C.W.B. Bezerra, L. Zhang, K. Lee, H. Liu, J. Zhang, Z. Shi, A.L.B. Marques, E.P. Marques, S. Wu, J. Zhang,"Novel carbon-supported Fe-N electrocatalysts synthesized through heat treatment of iron tripyridyltriazine complexes for the PEM fuel cell oxygen reduction reaction", *Electrochim. Acta*, vol. 53, pp. 7703-7710, Nov. 2008.

[23] S.L. Gojkovic, S. Gupta, R.F. Savinell, "Heat-treated iron(III) tetramethoxyphenylporphyrin chloride supported on high-area carbon as an electrocatalyst for oxygen reduction: Part III. Detection of hydrogen-peroxide during oxygen reduction", *Electrochim. Acta*., vol. 45, pp. 889-897, Dec. 1999.

[24] O. Contamin, C. Debiemme-Chouvy, M. Savy, G. Scarbeck, "O_2electroreduction catalysis: effects of sulfur addition on some cobalt macrocycles", *J. New. Mater. Electrochem. Syst*., Vol. 3, pp. 67-74, Jun. 2000.

[25] H. Schulenburg, S. Stankov, V. Schunemann, J. Radnik, I. Dorbandt, S. Fiechter, P. Bogdanoff, H. Tributsch, "Catalysts for the oxygen reduction from heat-treated Iron(III) Tetramethoxyphenylporphyrin chloride: structure and stability of active sites", *J. Phys. Chem. B*., vol. 107, pp. 9034-9041, Jul. 2003.

[26] C. Medard, M. Lefevre, J.P. Dodelet, F. Jaouen, G. Lindbergh, "Oxygen reduction by Fe-based catalysts in PEM fuel cell conditions: activity and selectivity of the catalysts obtained with two Fe precursors and various carbon supports", *Electrochim. Acta*, vol. 51, pp. 3202-3213, Apr. 2006.

[27] R. Baker, D.P. Wilkinson, J. Zhang, "Electrocatalytic activity and stability of substituted iron phthalocyanines towards oxygen reduction evaluated at different temperatures", *Electrochim. Acta*, vol. 53, pp. 6906-6919, Oct. 2008.

[28] S. Pylypenko, S. Mukherjee, T.S. Olson, P. Atanassov, "Non-platinum oxygen reduction electrocatalysts based on pyrolyzed transition metal macrocycles", *Electrochim. Acta*, vol. 53, pp. 7875-7883, Nov. 2008.

[29] U.I. Koslowski, I. Abs-Wurmbach, S. Fiechter, P. Bogdanoff, "Nature of the catalytic Centers of porphyrin-based electrocatalysts for the ORR: a correlation of kinetic current density with the site density of Fe-N_4 Centers", J. *Phys. Chem. C*, vol. 112, pp. 15356-15366, Sep. 2008.

[30] I. Herrmann, U.I. Kramm, S. Fiechter, P. Bogdanoff, "Oxalate supported pyrolysis of CoTMPP as electrocatalysts for the oxygen reduction reaction", *Electrochim. Acta*, vol. 54, pp. 4275-4287, Jul. 2009.

[31] V. Jalan, E.J. Taylor, "Importance of interatomic spacing in catalytic reduction of oxygen in phosphoric acid", *J. Electrochem. Soc*., vol. 130, pp. 2299-2302, Sep. 1983.

[32] M.T. Paffett, G.J. Berry, S. Gottesfeld, "Oxygen reduction at $Pt_{0.65}Cr_{0.35}$, $Pt_{0.2}Cr_{0.8}$ and roughened platinum", *J. Electrochem. Soc*., vol. 135, pp. 1431-1436, May 1988.

[33] B.C. Beard, P.N. Ross, "The structure and activity of Pt–Co alloys as oxygen reduction electrocatalysts", J. *Electrochem. Soc*., vol. 137, pp. 3368-3374, May 1990.

[34] T. Toda, H. Igarashi, H. Uchida, M. Watanabe, "Enhancement of the electroreduction of oxygen on Pt alloys with Fe, Ni, and Co", *J. Electrochem. Soc*., vol. 146, pp. 3750-3756, May 1999.

[35] T.R. Ralph, J.E. Keating, N.J. Collis, T.I. Hyde. ETSU Contract Report F/02/00038, 1997.

[36] D. Thompsett, in Vielstich W, Gasteiger H, Lamm A (Eds.), *Handbook of Fuel Cells-Fundamentals, Technology and Applications*, Wiley, Chichester, UK, 2003, pp. 467.

[37] U.A. Paulus, A. Wokaun, G.G. Scherer,T.J. Schmidt, V. Stamenkovic, N.M. Markovic, P.N. Ross, "Oxygen Reduction on Carbon Supported Pt-Ni and Pt-Co Alloy Catalysts", J. *Phys. Chem. B*, vol. 106, pp. 4181-4191, Mar. 2002.

[38] T. He, E. Kreidler, L. Xiong, J. Luo, C.J. Zhong, "Combinatorial screening and nano-synthesis of platinum binary alloys for oxygen electroreduction", *J. Electrochem. Soc.,* vol. 153, pp. A1637-A1643, Feb. 2006.

[39] E. Antolini, J.R.C. Salgado, E.R. Gonzalez, "The stability of Pt–M (M=first row transition metal) alloy catalysts and its effect on the activity in low temperature fuel cells: A literature review and tests on a Pt-Co catalyst", *J. Power. Sourc*., vol. 160, pp. 957-968, Oct. 2006.

[40] H.R. Colón-Mercado, H. Kim, B.N. Popov, "Durability study of Pt_3Ni_1 catalyst as cathode in PEM fuel cells", *Electrochem. Com*., vol. 6, pp. 795-759, Aug. 2004.

[41] H.R. Colón-Mercado, B.N. Popov, "Stability of platinum based alloy cathode catalysts in PEM fuel cells", *J. Power. Sourc*., vol. 155, pp. 253-263, Apr. 2006.

[42] G. Li, L. Hu, J.M. Hill, "Comparison of reducibility and stability of alumina-supported Ni catalysts prepared by impregnation and co-precipitation", *Appl. Catal. A*, vol. 301, pp.16-24, Feb. 2006.

[43] H. Wu, D. Wexler, G. Wang, "Pt_xNi alloy nanoparticles as cathode catalyst for PEM fuel cells with enhanced catalytic activity", *J. Alloys Comp*., vol. 488, pp. 195-198, Nov. 2009.

[44] Y.H. Cho, T.Y. Jeon, J.W. Lim, Y.H. Cho, M. Ahnb, N. Jung, S.J. Yoo, W.S. Yoon, Y.E. Sung, "Performance and stability characteristics of MEAs with carbon-supported Pt and Pt_1Ni_1 nanoparticles as cathode catalysts in PEM fuel cell", *Inter. J. Hydrogen. Ener*., vol. 36, pp. 4394-4399, Apr. 2011.

[45] C.S. Zignani, E. Antolini, E.R. Gonzalez, "Evaluation of the stability and durability of Pt and Pt–Co/C catalysts for polymer electrolyte membrane fuel cells", *J. Power Sourc*., vol. 182, pp. 83-90, Jul. 2008.

[46] B. Fang, B.N. Wanjala, J. Yin, R. Loukrakpam, J. Luo, X. Hu, J. Last, C.J. Zhong, "Evaluation of the stability and durability of Pt and Pt–Co/C catalysts for polymer electrolyte membrane fuel cells Electrocatalytic performance of Pt-based trimetallic alloy nanoparticle catalysts in proton exchange membrane fuel cells", *Inter. J. Hydro. Energ.*, vol. 37, pp. 4627-4632, Mar. 2012.

[47] W. Trongchuankij, K. Poochinda, K. Pruksathorn, M. Hunsom, "A study on novel combined processes for preparation of high performance Pt-Co/C electrocatalyst for oxygen reduction in PEM fuel cell", *Renew. Energ*., vol. 12, pp. 2839-2843, Dec. 2010.

[48] S. Thanasilp, M. Hunsom, "Effect of MEA fabrication techniques on the cell performance of Pt-Pd/C electrocatalyst for oxygen reduction in PEM fuel cell", *Fuel*, vol. 89, pp. 3847-3852, Dec. 2010.

[49] S. Thanasilp, M. Hunsom, "Preparation of a high performance Pt-Pd/C electrocatalyst coated membrane for ORR in PEM fuel cells via a combined process of impregnation and seeding: Effect of electrocatalyst loading on carbon support", *Electrochim. Acta*, vol. 56, pp. 1164- 1171, Jan. 2011.

[50] S. Thanasilp, M. Hunsom, "Effect of Pt: Pd atomic ratio in Pt-Pd/C electrocatalyst coated membrane on the electrocatalytic activity of ORR in PEM fuel cells", *Renew. Ener*., vol. 36, pp.1975-1801, Jun. 2011.

[51] C. Termpornvithit, N. Chewasatn, M. Hunsom, "Stability of Pt-Co/C and Pt-Pd/C based oxygen reduction reaction electrocatalysts prepared at a low temperature by a combined impregnation and seeding process in PEM fuel cells", *J. Appl. Electrochem*., vol. 42, pp.169-178, Mar. 2012.

[52] T. Ungar, J. Gubieza, G. Tichy, C. Pantea, T.W. Zerda, "Size and shape of crystallites and internal stresses in carbon blacks", *Compos. Part. A-Appl*., vol. 36, pp. 431-436, Apr.2005.

[53] Z.B. Wang, G.P. Yin, J. Zhang, Y.C. Sun, P.F. Shi, "Co-catalytic effect of Ni in the methanol electro-oxidation on Pt-Ru/C catalyst for direct methanol fuel cell", *Electrochim. Acta*., vol. 51, pp. 5691-5697, Aug. 2006.

[54] S. Liao, B. Li, Y. Li, *Physical characterization of electrocatalysts*, in *PEM fuel cell electrocatalysts and catalyst layers: Fundamental and applications*, J. Zhang, Ed., Springer-Verlag London Limited; 2008: pp 488.

[55] T. Lopes, E. Antolini, E.R. Gonzalez, "Carbon supported Pt-Pd alloy as an ethanol tolerant oxygen reduction electrocatalyst for direct ethanol fuel cells", *Int. J. Hydrogen Energy*, vol. 33, pp. 5563-5570, Oct. 2008.

[56] Z.B. Wang, G.P. Yin, P.F. Shi, Y.C. Sun, "Novel Pt-Ru-Ni/C catalysts for methanol electro-oxidation in acid medium", *Electrochem. Solid-State Lett*., vol. 9, pp. A13-A15, Nov. 2006.

[57] J.J. Van Der Klink, "NMR spectroscopy as a probe of surfaces of supported metal catalysts", *Adv. Catal*., Vol. 44, pp. 1-117, Apr. 1999.

[58] K. Kinoshita, *Electrochemical oxygen technology*, John Wiley & Sons, Inc. 1992.

[59] J. O'M. Bockris, A. Damjanovic, J. McHardy, ThirdInternatoinal Symposium on Fuel Cells (TroisiemesJournees Internationales D'etudes de Piles a Combustibles), p.15 Presses AcademiqueEuropeennes, Brussels, 1969. Proceedings of a conference held under joint sponsor of SERAI and COMASCI, Brussels, June 16-20, 1969.

[60] E.Antolini, L. Giorgi, A. Pozio, E. Passalacqua, "Influence of Nafion loading in the catalyst layer of gas-diffusion electrodes for PEFC", *J. Power Sourc*., vol. 77, pp.136-142, Feb. 1999.

[61] E. Rios, S. Abarca, P. Daccarett, P.N. Cong, D. Martel, J.F. Marco, J.R. Gancedo, J.R. Gautier, "Electrocatalysis of oxygen reduction on $Cu_xMn_{3-x}O_4$ ($1.0 \leq x \leq 1.4$) spinel particles/polypyrrole composite electrodes", *Inter. J. Hydro. Energ*., vol. 33, pp. 4945-4954, Oct. 2008.
[62] J. Larminie, A. Dick, *Fuel cell systems explained*. 2nd edition. Chichester: John Wiley & Sons, 2003.
[63] H. Lv, S. Mu, N. Cheng, M. Pan, "Nano-silicon carbide supported catalysts for PEM fuel cells with high electrochemical stability and improved performance by addition of carbon", *Appl. Catal. B*, vol. 100, pp. 190-196, Oct. 2010.
[64] S.Y. Huang, P. Ganesan, B.N. Popov, "Titania supported platinum catalyst with high electrocatalytic activity and stability for polymer electrolyte membrane fuel cell", *Appl. Catal. B*, vol. 102, pp. 71-77, Feb. 2011.
[65] U.A. Paulus, A. Wokaun, G.G. Scherer, T.J. Schmidt, V. Stamenkovic, N.M. Markovi, P.N. Ross, "Oxygen reduction on high surface area Pt-based alloy catalysts in comparison to well defined smooth bulk alloy electrodes", *Electrochim. Acta*, vol. 47, pp. 3787-3798, Aug. 2002.
[66] G. Prentice, *Electrochemical Engineering Principles*, Prentice Hall Inc., New Jersey, 1991.
[67] P. Yu, M. Pemberton, P. Plasse, Plasse P., "PtCo/C cathode catalyst for improved durability in PEMFCs", *J. Power Sourc*., vol. 144, pp. 11-20, Jun. 2005.
[68] J. Lobato, P. Cañizares, M.A. Rodrigo, J.J. Linares, "PBI-based polymer electrolyte membranes fuel cells: Temperature effects on cell performance and catalyst stability", *Electrochim. Acta*, vol. 52, pp. 3910-3920, Mar. 2007.
[69] P.J. Ferreira, G.J. la O', Y. Shao-Horn, D. Morgan, R. Makharia, S. Kocha, "Instability of Pt/C electrocatalysts in proton exchange membrane fuel cells", *J. Electrochem. Soc*., vol. 152, pp. A2256-A22571, Oct. 2005.
[70] T.R. Ralph, M.P. Hogarth, "Catalysis for low temperature fuel cells part I the cathode challenges", *Plat. Met. Rev*., vol. 46, 3-14, Jan. 2002.
[71] H.A. Gasteiger, S.S. Kocha, B. Sompalli, F.T. Wagner, "Activity benchmarks and requirements for Pt, Pt-alloy, and non-Pt oxygen reduction catalysts for PEMFCs", *Appl. Catal. B*., vol. 56, pp. 9-35, Mar. 2005.
[72] C.H. Cho, B. Choi, Y.H. Cho, H.S. Park, Y.E. Sung, "Pd-based PdPt(19:1)/C electrocatalyst as an electrode in PEM fuel cell", *Electrochem. Com*., vol. 9, pp. 378-381, Mar. 2007.
[73] M. Watanabe, K. Tsurumi, T. Mizukami, T. Nakamura, P. Stonehart, "Activity and stability of ordered and disordered Co-Pt alloys for phosphoric acid fuel cells", *J. Electrochem. Soc*., vol. 141, pp. 2659-2668, May 1994.
[74] D.C. Huang, P.J. Yu, F.J. Liu, S.L. Huang, K.L. Hsueh, Y.C. Chen, C.H. Wu, W.C. Chang, F.H. Tsau, "Effect of dispersion solvent in catalyst ink on proton exchange membrane fuel cell performance", *Int. J. Electrochem*. Sci., vol. 6, pp. 2551-2565, Jul. 2011.